Tectonics

RESEARCH ARTICLE
10.1029/2020TC006180

Key Points:
- First low-temperature thermochronology (LTT) study of the Bunger Hills basement in East Antarctica
- LTT data record widespread cooling and exhumation of East Antarctic basement associated with Pangea-wide extension
- Large-scale topographic framework established during intracontinental extension has influenced long-term landscape evolution of East Antarctica

Supporting Information:
- Supporting Information S1
- Table S1

Correspondence to:
A. Maritati,
alessandro.maritati@utas.edu.au

Citation:
Maritati, A., Danišík, M., Halpin, J. A., Whittaker, J. M., & Aitken, A. R. A. (2020). Pangea rifting shaped the East Antarctic landscape. *Tectonics*, *39*, e2020TC006180. https://doi.org/10.1029/2020TC006180

Received 4 MAR 2020
Accepted 4 AUG 2020
Accepted article online 7 AUG 2020

Pangea Rifting Shaped the East Antarctic Landscape

Alessandro Maritati[1], Martin Danišík[2], Jacqueline A. Halpin[1], Joanne M. Whittaker[1], and Alan R. A. Aitken[3]

[1]Institute for Marine and Antarctic Studies, University of Tasmania, Hobart, Tasmania, Australia, [2]John de Laeter Centre/The Institute for Geoscience Research, Curtin University, Perth, Western Australia, Australia, [3]School of Earth Sciences, University of Western Australia, Perth, Western Australia, Australia

Abstract East Antarctica remains one of the few continental regions on Earth where an understanding of the origin and causal processes responsible for topographic relief is largely missing. Low-temperature thermochronology studies of exposed Precambrian basement revealed discrete episodes of cooling and denudation during the Paleozoic–Mesozoic; however, the significance of these thermal events and their relationship to topography across the continental interior remains unclear. Here we use zircon and apatite (U-Th)/He thermochronology to resolve the low-temperature thermal evolution of a poorly exposed section of East Antarctic basement in the Bunger Hills region and gain insights into the chronology and style of landscape evolution across East Antarctica. Thermal history modeling results indicate that Precambrian basement in the Bunger Hills region experienced a distinct cooling episode during the Late Paleozoic–Triassic, which we relate to ~2–4 km of regional exhumation associated with intracontinental rifting, followed by a second episode of localized cooling and ≤1 km exhumation during the Late Jurassic–Cretaceous separation of India from East Gondwana. These findings, combined with existing thermochronological and tectonic evidence, support a continent-scale denudation event associated with uplift and exhumation of large sections of Precambrian basement during Late Paleozoic–Triassic Pangea-wide intracontinental extension. By contrast, continental extension associated with the Jurassic–Cretaceous breakup of East Gondwana resulted in significant denudation only locally in regions west of the Bunger Hills. We propose that the combined effects of these Paleozoic–Mesozoic tectonic events had a profound impact on the topography across the East Antarctic interior and influenced the long-term landscape evolution of East Antarctica.

1. Introduction

The origin of topographic relief in old and tectonically stable continental interiors is a long-standing problem in continental dynamics (e.g., Ferraccioli et al., 2011; Hu et al., 2018). East Antarctica comprises one of the largest composite Precambrian shields on Earth and is a chief example of a vast continental region with topographic variability akin to tectonically active regions (Creyts et al., 2014). The most significant morphological variations across East Antarctica broadly correlate with the Precambrian domains of Australo-Antarctica and Indo-Antarctica, which amalgamated during the ~600–550 Ma assembly of Gondwana (e.g., Mulder et al., 2019). Despite preserving Precambrian crust with broadly similar thicknesses (Pappa et al., 2019), these two domains exhibit remarkably distinct hypsometry (O'Donnell & Nyblade, 2014; Figure 1a). Indo-Antarctica possesses elevated, high-relief topography above the global average with narrow and deep rift basins (Ferraccioli et al., 2011). By contrast, the Australo-Antarctic domain comprises smoother topography at longer wavelengths and features large subglacial sedimentary basins where the vast majority of topography is below sea level (Aitken et al., 2014; Frederick et al., 2016; Maritati et al., 2016). Proposed models for the origin and long-term evolution of topography of ancient cratonic regions include high-standing passive margin formation during continental breakup (e.g., southern Africa; Wildman et al., 2016), large-scale denudation of Phanerozoic cover (e.g., Yilgarn Craton; Weber et al., 2005), and far-field deformation transmitted from collisional plate interactions (e.g., Canadian Shield; Pinet, 2016). However, an understanding of the causal processes responsible for the large-scale hypsometric variability across East Antarctica remains largely missing due to its poorly understood Phanerozoic landscape evolution.

Low-temperature (<300°C) thermochronology (LTT) has been widely used to quantify spatial and temporal patterns of cooling in continental settings, which in turn can provide constraints on the rates and

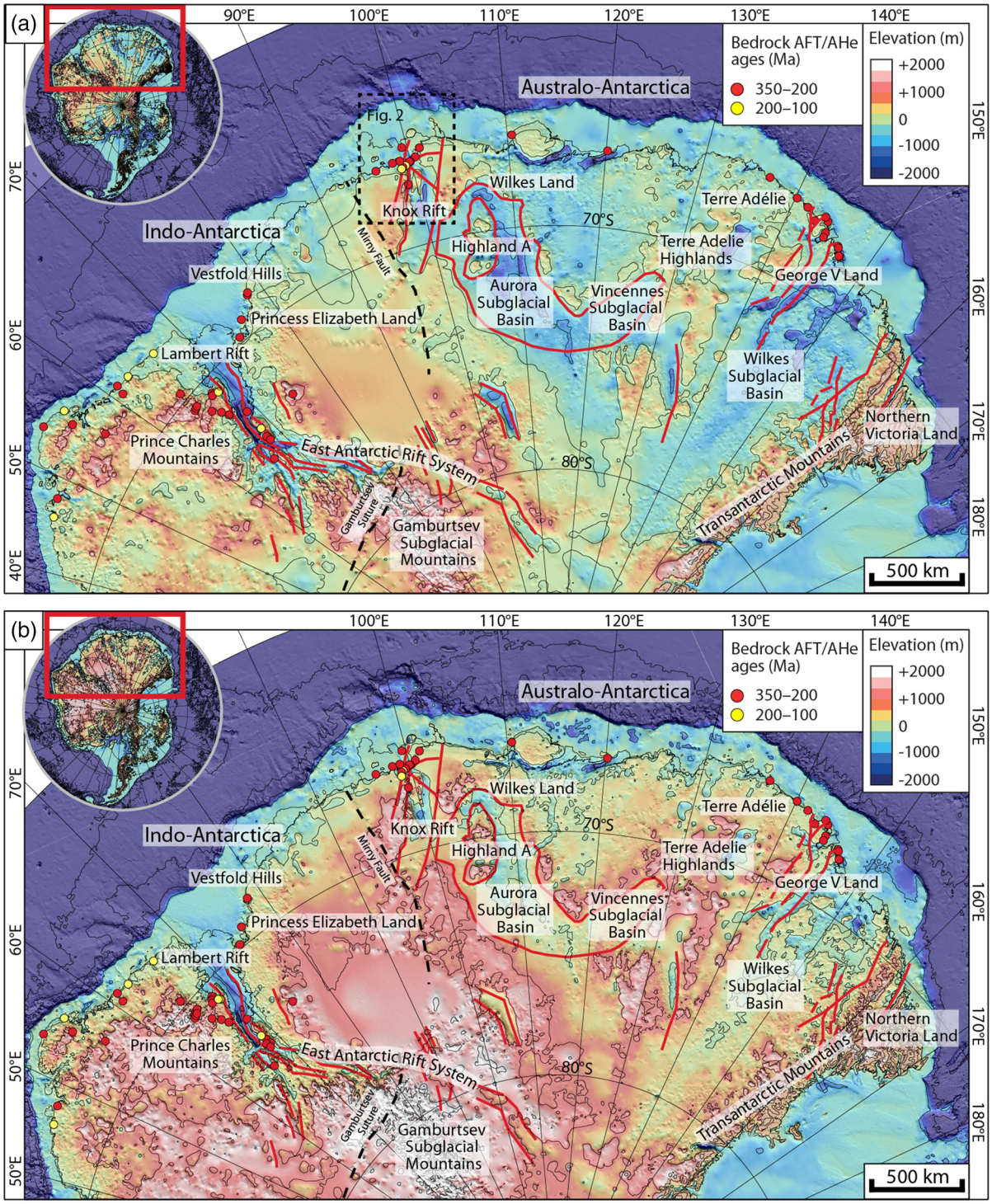

Figure 1. (a) Present-day bedrock topography of the Indo-Antarctic and Australo-Antarctic sectors of East Antarctica from BedMachine (Morlighem et al., 2020); (b) bedrock topography after isostatic rebound due to the removal of the present-day ice load (Paxman, Jamieson, Hochmuth, et al., 2019). Bedrock elevations on both grids are contoured at 1 km intervals. Colored circles show published bedrock AFT and AHe data from the Lambert Rift area (Arne, 1994; Lisker et al., 2003; Lisker, Gibson, et al., 2007), Vestfold Hills (Lisker, Wilson, & Gibson, 2007), and Terre Adélie/George V Land (Lisker & Olesch, 2003; Rolland et al., 2019) as well as reconnaissance AFT data of Arne et al. (1993). Sedimentary basin-bounding faults in the EARS (Ferraccioli et al., 2011), Knox Rift (Maritati et al., 2016), Aurora and Vincennes Subglacial Basins, (Aitken, Roberts, et al., 2016), Wilkes Subglacial Basin (Paxman, Jamieson, Ferraccioli, et al., 2019, and references therein) are highlighted in red; dashed black lines correspond to the inferred path the Mirny Fault (Daczko et al., 2018) and Gamburtsev Suture (Ferraccioli et al., 2011), which together represent the paleoplate boundary between Indo-Antarctica and Australo-Antarctica (Mulder et al., 2019); dashed box in panel (a) indicates a detail of the Bunger Hills region shown in Figure 2.

mechanisms of landscape evolution (Kohn & Gleadow, 2019). Existing LTT data from Precambrian basement outcrops in the Indo-Antarctic and Australo-Antarctic domains suggest major cooling of East Antarctic basement during the Paleozoic–Mesozoic (Figure 1); however, the significance of these observed Paleozoic–Mesozoic tectonothermal events across interior East Antarctica, and any link in establishing the different topographic response of each domain, remains elusive. In the Indo-Antarctic domain, apatite fission track (AFT) data from basement rocks in the northern Prince Charles Mountains (PCM) and Vestfold Hills record cooling associated with up to 5 km of basement exhumation during two discrete phases of continental rifting in the Lambert Rift (Arne, 1994; Lisker et al., 2003; Lisker, Gibson, et al., 2007; Lisker, Wilson, & Gibson, 2007) and broader East Antarctic Rift System (EARS; Ferraccioli et al., 2011) in the Late Paleozoic–Triassic (~310–200 Ma) and Cretaceous (~120–100 Ma). In the Australo-Antarctic domain west of the Transantarctic Mountains (TAM), AFT and apatite (U-Th)/He (AHe) data record a single Late Paleozoic–Triassic cooling event between ~350 and 200 Ma. This cooling has been interpreted to result from 3–4 km denudation triggered by either tectonic uplift synchronous with extension in the Wilkes Subglacial Basin (Lisker & Olesch, 2003), or denudation during large-scale glacial erosion of the Late Paleozoic Ice Age (Rolland et al., 2019). Investigations based on geophysical data and plate reconstructions have also suggested significant Cretaceous–Cenozoic onshore extensional tectonic activity in the interior of the Australo-Antarctic domain associated with plate divergence during the breakup of East Gondwana (Aitken et al., 2014; Eagles, 2019; Maritati et al., 2016) or intraplate strike-slip tectonics (e.g., Cianfarra & Maggi, 2017).

In this paper, we seek to establish a link between LTT data and Phanerozoic continent-scale geodynamic processes and the generation of variable hypsometry across East Antarctica. We use new (U-Th)/He data on zircon and apatite to reconstruct the low-temperature thermal evolution of Precambrian basement in the Bunger Hills region, located near the transition between high-relief regions of Indo-Antarctica and the low-lying subglacial basins of Australo-Antarctica. Our new results, combined with existing thermochronological, stratigraphic, and tectonic constraints, provide evidence for a major denudational event across the East Antarctic interior associated with Late Paleozoic–Triassic intracontinental extension. We interpret these new results in the context of their Pangea-wide tectonic setting and discuss the influence of topographic development at this stage on the landscape evolution of East Antarctica.

2. The Bunger Hills Region

Located in the western Wilkes Land sector of East Antarctica, the Bunger Hills region features a series of Precambrian–Early Cambrian coastal basement outcrops and remote inland nunataks, which together comprise the largest ice-free oasis in the western Australo-Antarctic domain (Tucker et al., 2020; Figure 2). These outcrops lie east of the inferred crustal boundary between Indo-Antarctica and Australo-Antarctica and record a complex tectonic history that culminated in the suturing of Australo-Antarctica and Indo-Antarctica along the Ediacaran–Cambrian Kuunga Orogen (Mulder et al., 2019). Exposed basement in the region forms the western flank of the Knox Rift, a Phanerozoic rift basin that is characterized solely from geophysical data (Maritati et al., 2016; Figure 2). The Knox Rift overprints basement and exerts a key influence on the regional topographic relief: While its flanks exhibit elevated (~1,200 m) and rugged topography, its central depression has focused erosion from the Denman and Scott Glaciers, two of the largest ice streams in the region, and hosts the deepest continental trench on Earth (Morlighem et al., 2020). The timing of extension in the Knox Rift, as well as the age of the sedimentary infill, is poorly known; plate reconstructions overall support a tectonic correlation with the Paleozoic–Mesozoic Perth Basin of western Australia within Gondwana. However, different phases of extension have been proposed in the Late Paleozoic–Triassic coeval with the Lambert Rift and EARS (Veevers, 2018) and during the Late Jurassic–Cretaceous separation of India from East Gondwana (Maritati et al., 2016).

3. Methods

3.1. (U-Th)/He Analysis

(U-Th)/He analysis was performed at the John de Laeter Centre (Curtin University, Perth). A summary of the samples used is given in the supporting information (Table S1). Apatite and zircon crystals of suitable size, shape, and quality were handpicked from mineral concentrates or plucked from epoxy mounts,

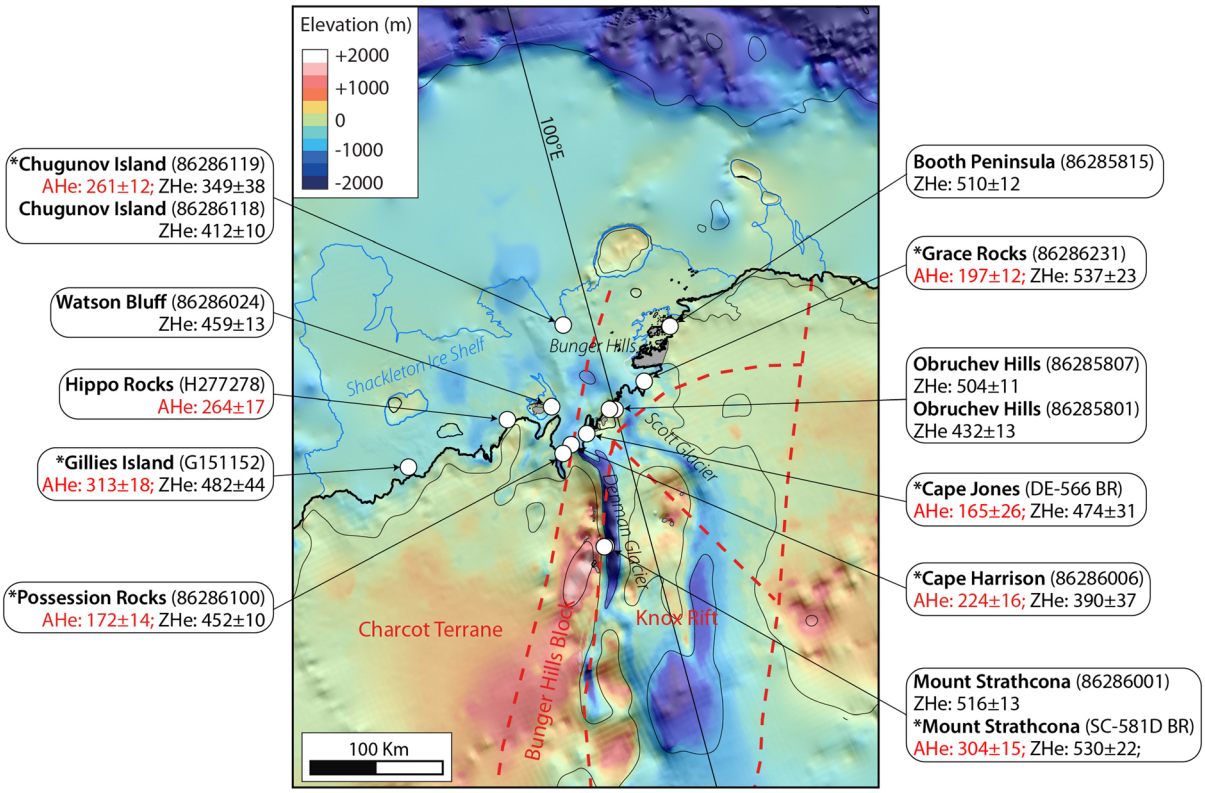

Figure 2. Bedrock topography map of Bunger Hills region showing exposed bedrock (gray areas), coastline (solid black line), and topographic contours at 1 km intervals (thin black lines). Simplified regional tectonic lineaments from Maritati et al. (2016) are shown as dashed red lines. The basement domains of the Bunger Hills Block and Charcot Terrane form the western flank of the Knox Rift. White circles represent location of Precambrian basement samples. For each sample, the weighted mean AHe (red) and ZHe ages (black) and respective 1σ uncertainties in Ma are indicated. Asterisks indicate samples for which modeled time-temperature (*t-T*) diagrams are presented in Figure 3.

previously used for U-Pb geochronology. Selected grains were then photographed and measured for dimensions to calculate alpha ejection correction factor and individually loaded in Pt (apatite) and Nb microtubes (zircon). Radiogenic ^{4}He was extracted at ~1250°C (zircon) or ~960°C (apatite) under ultrahigh vacuum using a diode laser, and its amount was determined by isotope dilution using ^{3}He spike on a Pfeiffer Prisma QMS 200 mass spectrometer. Following the ^{4}He measurements, microtubes containing the crystals were retrieved from the laser cell, spiked with ^{235}U and ^{230}Th, and dissolved in acids following the procedure of Evans et al. (2005), and the solutions were analyzed by isotope dilution for U and Th and by external calibration for Sm on an Agilent 7500 ICP-MS. Total analytical uncertainty of uncorrected (U-Th)/He ages was calculated by propagating uncertainties of U, Th, Sm, and He measurements. The uncorrected zircon (U-Th)/He (ZHe) and AHe ages were corrected for α-ejection (Ft correction) after Farley et al. (1996), whereby a homogenous distribution of U, Th, and Sm was assumed for the crystals. The accuracy of (U-Th)/He dating procedure was monitored by replicate analyses of Fish Canyon Tuff zircon (n = 11) and Durango apatite (n = 12) measured over the period of this study as internal standards, yielding mean (U-Th)/He ages of 29.2 ± 1.0 and 31.8 ± 1.1 Ma, respectively. These ages are in good agreement with the reference ages of 28.3 ± 1.3 Ma (Fish Canyon Tuff; Reiners et al., 2002) and 31.13 ± 1.01 Ma (Durango; McDowell et al., 2005). (U-Th)/He analytical results are presented in Table S2.

3.2. Time-Temperature Modeling of LTT Data

Inverse thermal history modeling was carried out using HeFTy v1.9 software (Ketcham, 2005) to find time-temperature (*t-T*) paths that that can reproduce measured thermochronological data and test plausible geological evolution scenarios. Only samples for which both zircon and apatite (U-Th)/He data are available were modeled. The models were parameterized as follows: Diffusion kinetic parameters for zircon and

apatite (U-Th)/He systems were adopted from Reiners et al. (2004) and Farley (2000), respectively; radii of the spherical diffusion domains were based on the measured size of the analyzed crystals and calculated equivalent sphere size; measured single-grain ages that were closest to the population mean age were modeled as representative for the samples. A Monte Carlo search method with 10,000 search tries was applied to find thermal trajectories that could reconcile the predefined parameters and constraints. "Acceptable" and "good" thermal paths were defined as having a goodness of fit (GOF) of >0.05 and >0.5, respectively.

4. Results and Interpretation

4.1. Zircon and Apatite (U-Th)/He Thermochronology Results

We report 72 zircon and 57 apatite single-grain (U-Th)/He ages from 14 basement outcrop samples from the western flank of the Knox Rift (Figure 2 and Table S2). Reproducibility of replicates within samples is good with the majority of single-grain ages overlapping within uncertainty. Our analysis shows that ZHe ages are in the range of ~537–365 Ma. In contrast, AHe ages are systematically younger than ZHe ages in each sample and range between ~313 and 165 Ma. AHe ages are consistent with an AFT age of 243 ± 13 Ma previously reported for a single sample from the Bunger Hills (Arne et al., 1993) and overall confirm the Late Paleozoic–Mesozoic age trend of AHe and AFT basement ages in the Indo-Antarctic and Australo-Antarctic domains. Sampling resolution is limited to mainly coastal and low-elevation basement outcrops hindering identification of spatial age trends across the Bunger Hills region. However, we note that AHe ages around the Denman and Scott glaciers (i.e., Possession Rocks, Cape Harrison, Cape Jones, and Grace Rocks) appear to form a cluster of relatively younger Triassic–Jurassic (224–165 Ma) ages while progressively older Late Carboniferous–Permian AHe ages occur to the west (Gillies Island and Hippo Rocks), south (Mount Strathcona), and north (Chugunov Island).

4.2. Phanerozoic Thermal History of the Bunger Hills Region

We explore the implications of the (U-Th)/He data for the Phanerozoic thermal history of Precambrian basement in the Bunger Hills region using *t-T* modeling of seven samples for which we have both ZHe and AHe data. To extract realistic thermal histories, we have incorporated in our models a framework of *t-T* constraints based on available geological constraints: In all model runs, the end of the *t-T* path was set to −10°C according to the present-day annual mean surface temperature recorded at the Antarctic station of Casey; the starting point was set to a temperature of 500°C at 550 Ma reflecting minimum peak temperatures during the Kuunga orogenic event. Although not exposed in outcrop, we presume that the contact between Precambrian basement and sedimentary rocks at the base of the Knox Rift likely forms an erosional unconformity. A similar erosional surface separating Precambrian basement rocks from the overlying glaciogenic Latest Carboniferous–Permian sedimentary sequences exists in the conjugate south Perth Basin in Australia (Norvick, 2004). We therefore incorporate this constraint in our models and force a cooling to near-surface temperatures ($T = -10$–20°C) between 350 and 300 Ma. Using these three fixed constraints, we model three different scenarios to test presence and magnitude of reheating during proposed extensional phases of the Knox Rift in the Late Paleozoic–Triassic (Veevers, 2018), Late Jurassic–Cretaceous (Maritati et al., 2016), and in both of these periods. Accordingly, for these periods we introduce additional constraints permitting temperatures of 30–220°C reflecting near-surface temperature conditions and maximum temperature limit of He retention in zircon, respectively. More specifically, the Late Paleozoic–Triassic extension was implemented by forcing reheating to temperatures between 30°C and 220°C during the Late Paleozoic–Triassic (300–200 Ma) from Carboniferous near-surface temperatures. Late Jurassic–Cretaceous extension was implemented by forcing the samples to a surface temperature of ~20°C in the Early Jurassic (200–160 Ma) from Carboniferous near-surface temperatures, followed by reheating between 30°C and 220°C in the Late Jurassic–Cretaceous (160–120 Ma). Finally, a two-stage extension scenario where Late Paleozoic–Triassic extension is followed by rapid cooling in the Late Triassic–Early Jurassic and renewed reheating in the Late Jurassic–Cretaceous was also implemented by combining the constraints of the two previous scenarios. In all models, timing of extension is calibrated to the conjugate Perth Basin which possesses well-documented stratigraphic and kinematic evidences for both a Late Paleozoic–Triassic and a Late Jurassic–Cretaceous extensional phase (Norvick, 2004). A summary of *t-T* modeling results is given in Figure 3 and in the supporting information (Table S3).

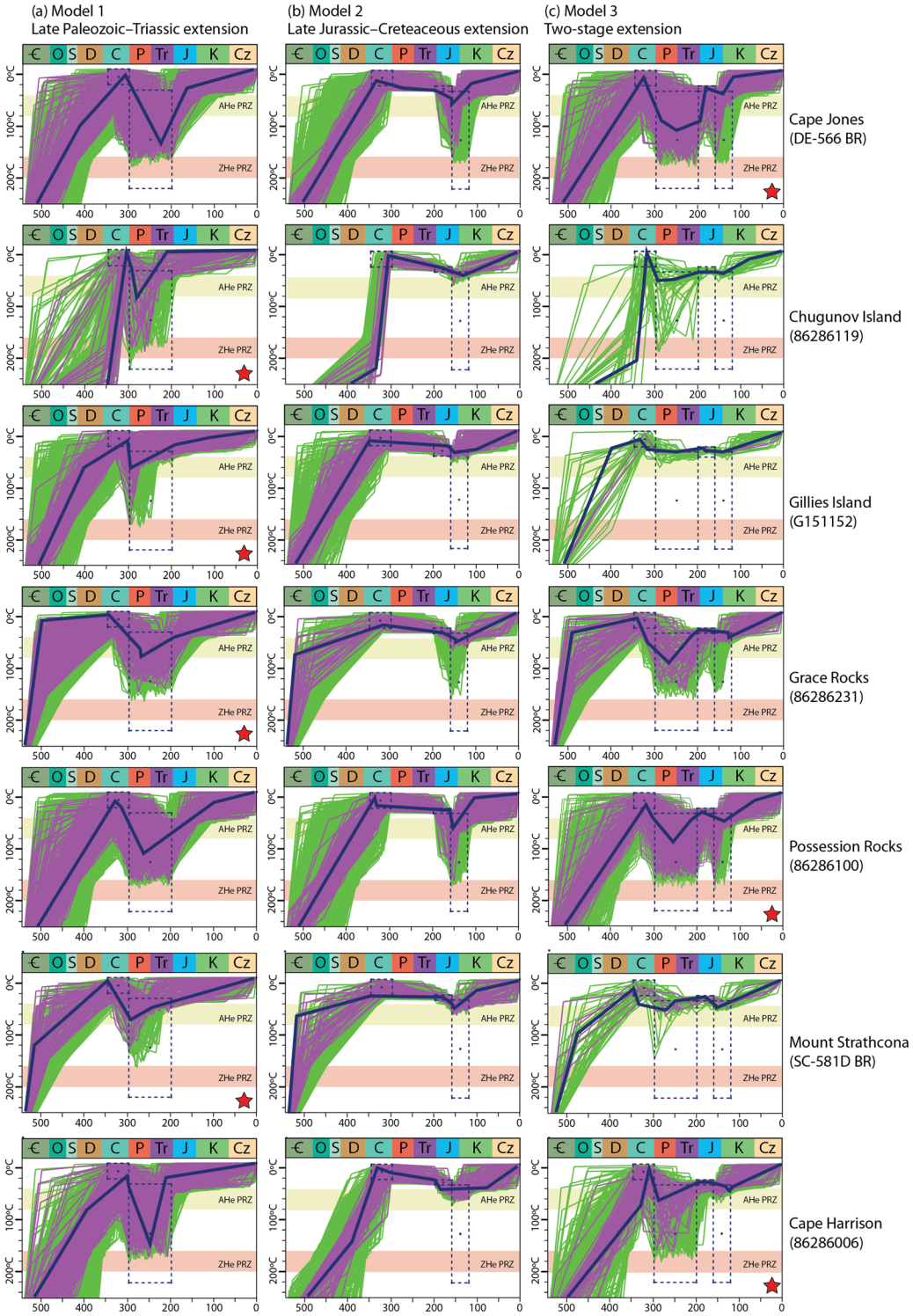

Figure 3. Modeled thermal histories of seven basement samples from the Bunger Hills region displayed as time-temperature (*t-T*) diagrams. *t-T* diagrams are shown for each of the three model scenarios (a–c). In each *t-T* diagram, green and pink lines indicate "acceptable" (GOF > 0.05) and "good" (GOF > 0.5) thermal trajectories, respectively; thick blue lines represent the best fit trajectories; dashed boxes represent predefined *t-T* constraints; red star indicates the preferred model scenario for each sample. Approximate temperature ranges of AHe partial retention zone (AHe PRZ, 40–80°C; Farley, 2000) and ZHe partial retention zone (ZHe PRZ, 160–200°C; Reiners et al., 2004) are also shown. Measured and modeled ZHe and AHe ages with their respective GOF values for each set of models are indicated in Table S3 in the supporting information.

Thermal history models reveal that cooling of Precambrian basement in the Bunger Hills region to near-surface temperatures (~30°C) after the Kuunga Orogeny 350–300 Ma must have been followed by at least one reheating-cooling episode between the Late Paleozoic and/or Cretaceous. Given that all our samples are located on the western rift flank in regions that are free of sedimentary cover and likely did not experience substantial (km-scale) burial of sedimentary rocks (Maritati et al., 2016), we infer the reheating-cooling episodes were achieved by an increase in the regional geothermal gradient due to rift-related processes.

Thermochronology data for Gillies Island, Mount Strathcona, Grace Rocks, and Chugunov Island are best reproduced with a single reheating-cooling episode in the Late Paleozoic–Triassic reaching peak temperatures of ~90–60°C (Figure 3a). Paleogeothermal gradient estimates during extension in the Lambert Rift suggest an increase to ~30°C km^{-1} in the vicinity of the rift from a stable geothermal gradient of 19–20°C km^{-1} (Lisker et al., 2003). Similar estimates may be also reasonable during extension in the Knox Rift, where a geothermal gradient increase of similar magnitude (~10°C km^{-1}) would explain the resetting of AHe systems from near-surface temperatures in basement samples on the western rift flank (Figure 4a). Cooling of basement samples at Gillies Island, Mount Strathcona, Grace Rocks, and Chugunov Island was most likely produced by thermal relaxation of the rift-related anomaly; for any assumed geothermal gradient estimates between 20°C km^{-1} and 30°C km^{-1}, cooling must have been associated with a maximum exhumation and erosion of ~ 2–4 km of basement overburden at these localities (Figure 4a). Thermal models for these samples also indicate that a phase of reheating between ~160 and 120 Ma is unlikely as samples could not exceed temperatures of 40°C in both the Late Jurassic–Cretaceous extension and two-stage extension scenarios (Figures 3b and 3c).

Thermal histories for Cape Jones, Cape Harrison, and Possession Rocks permit reheating to temperatures greater than 40°C in the Late Paleozoic–Triassic, Late Jurassic–Cretaceous, or in both these intervals (Figures 3a–3c). Maximum paleotemperatures in models simulating a single reheating phase in the Late Paleozoic–Triassic range between 160°C and 120°C and require the development of a substantially elevated paleogeothermal gradient in excess of 60°C km^{-1} (Figure 3a). The two-stage extension scenario, in contrast, suggests lower Late Paleozoic–Triassic maximum paleotemperatures of ~90–60°C, which are consistent with those extracted from the Gillies Island, Mount Strathcona, Grace Rocks, and Chugunov Island samples and indicate ~2 km of post-Permian basement exhumation (Figures 3c and 4b). Furthermore, it allows for a second phase of modest rift-related reheating of basement to temperatures of ~40–50°C from Late Jurassic surface temperatures of 20°C in the Late Jurassic–Cretaceous, which indicates ≤1 km of post-Cretaceous basement exhumation (assuming a paleogeothermal gradient of ~20–30°C km^{-1}) in addition to ~2 km of Permian–Jurassic basement exhumation (Figure 4b).

In summary, thermal history models support regional cooling to Late Paleozoic near-surface temperatures after the Kuunga tectonothermal event, followed by reheating and cooling through ~90–60°C during Late Paleozoic–Triassic triggered by the rift-related thermal anomaly and exhumation of Precambrian basement on the western rift flank. The magnitude of cooling suggests ~2–4 km exhumation for reasonable amounts of assumed paleogeothermal gradients. A second thermal event in the Late Jurassic–Cretaceous and minor exhumation of ≤1 km is identified locally in three samples near the coast and may be associated with localized reactivation of rift structures during the onset of early rifting between Antarctica, Australia, and India. These results are consistent with the establishment of topographic relief during continental extension and associated rift flank basement uplift predominantly in the Late Paleozoic–Triassic, with additional localized uplift during the Late Jurassic–Cretaceous in the Denman Glacier area.

5. Discussion

5.1. Phanerozoic Thermal History of the Indo-Antarctic and Australo-Antarctic Basement

Inversion of thermochronological data allowed to interrogate the low-temperature thermal history of Precambrian basement in the Bunger Hills region, providing key constraints to understand the pattern and magnitude of cooling, and to reconstruct the morphotectonic evolution of this sector of East Antarctica during the Phanerozoic. Circa 313–200 Ma AHe ages from the Bunger Hills region are consistent with the predominantly Late Paleozoic–Triassic age trend recorded by previously published AFT and AHe thermochronometers in the Indo-Antarctic and Australo-Antarctic domains, supporting a single

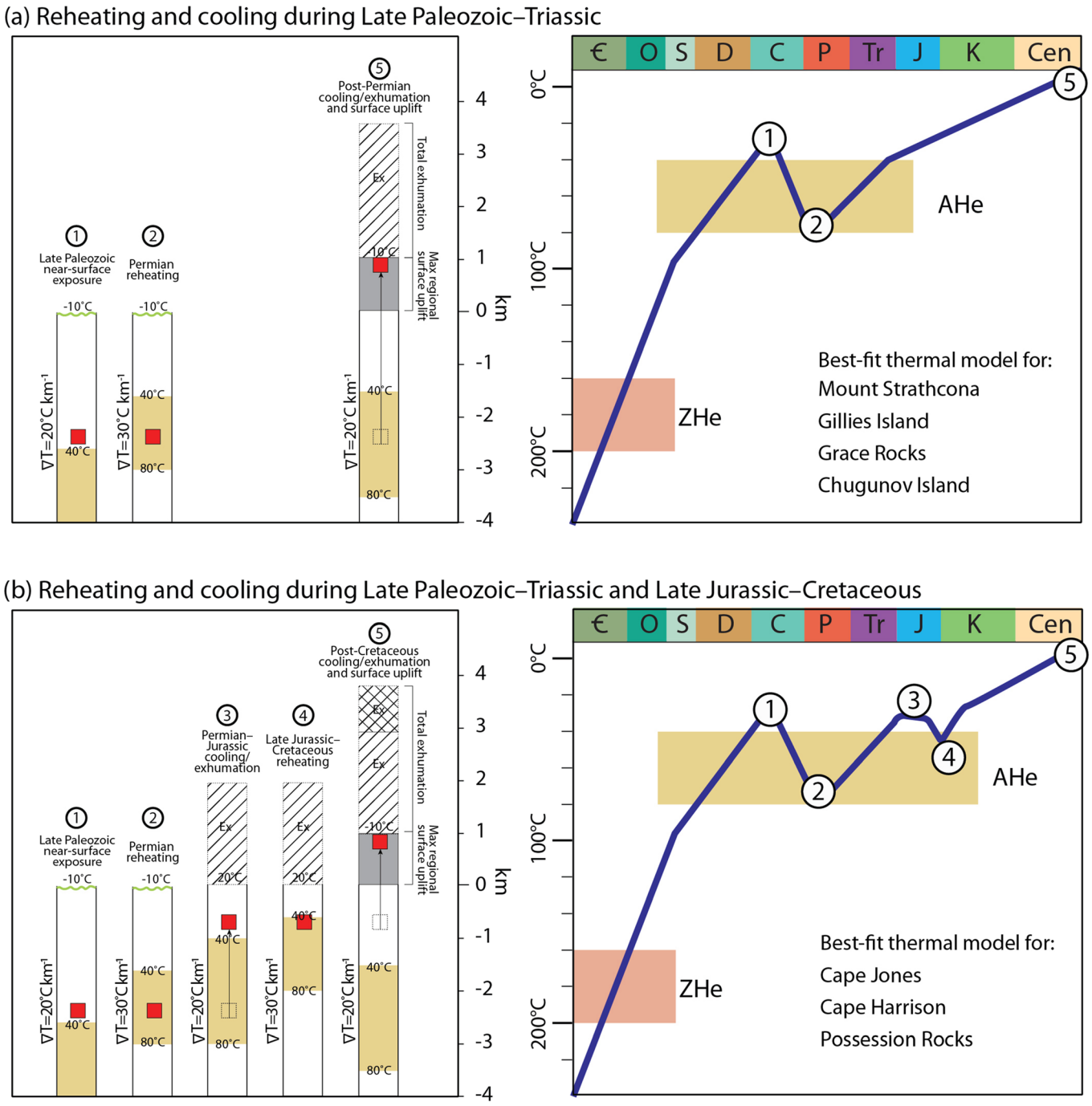

Figure 4. Schematic representation of the relationship between reheating-cooling episodes of basement samples (red squares) and rock uplift with respect to best fit time-temperature (*t-T*) trajectories modeled for the (a) Late Paleozoic–Triassic extension scenario and (b) two-stage extension scenario. Rock uplift equals to the amount of exhumation (Ex) plus the amount of surface uplift (gray shading) with respect to a reference surface (England & Molnar, 1990). Surface temperature used in *t-T* models and approximate temperature ranges of AHe partial retention zone (AHe PRZ, 40–80°C, brown fill; Farley, 2000) and ZHe partial retention zone (ZHe PRZ, 160–200°C, red fill; Reiners et al., 2004) are also shown.

large-scale cooling event of East Antarctic basement from temperatures of at least 120°C (upper limit of AFT partial annealing zone [PAZ]; Wagner et al., 1989). Our thermal models suggest that the cooling pattern of Precambrian basement in the Bunger Hills region requires ~2–4 km exhumation during Late Paleozoic–Triassic (~300–200 Ma) intracontinental extension in the Knox Rift. This interpretation is consistent with

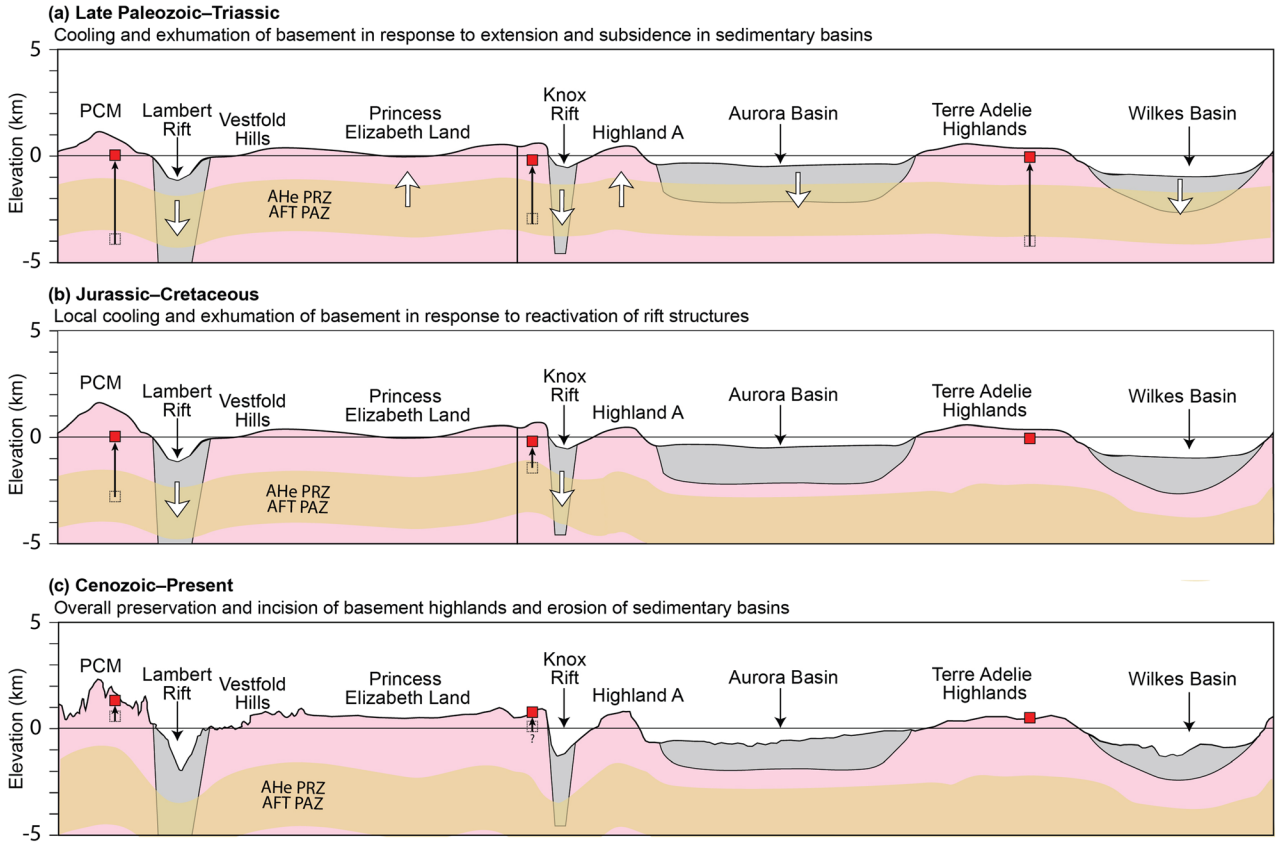

Figure 5. Conceptual cartoon illustrating the interpreted morphotectonic evolution of the Indo-Antarctic and Australo-Antarctic domains. (a) Exhumation of Precambrian basement in response to widespread extension and subsidence in sedimentary basins during Pangea-wide rifting. (b) Exhumation of Precambrian basement in response to reactivation of structures during the Jurassic–Cretaceous breakup of East Gondwana (i.e., Lambert and Knox Rifts). (c) Slow cooling of uplifted basement to present-day surface temperatures and overall preservation of high-standing topographic features throughout the Cenozoic. In each panel, red squares represent the position of representative samples as inferred from LTT data. Approximate temperature ranges of the combined AHe PRZ and AFT PAZ (40–120°C) are shown in each panel. For accuracy, we show the possible effects of increased geothermal gradient during rifting phases and the influence of finite-amplitude topography on the morphology of the combined AHe PRZ and AFT PAZ in each schematic profile. Elevations in the Late Paleozoic–Triassic and Jurassic–Cretaceous panels are approximate.

the timing and style of Late Paleozoic–Triassic cooling and exhumation associated with extension in the Lambert Rift (Lisker et al., 2003), and the Wilkes Subglacial Basin (Lisker & Olesch, 2003), and indicates that the East Antarctic basement between the Lambert Rift and George V Land may have been part of a single denudational system. We therefore suggest that the uplift and erosion of large sections of Precambrian basement during Late Paleozoic–Triassic intracontinental extension provide an explanation for the cooling pattern of AFT and AHe systems in Precambrian basement rocks across both Indo-Antarctica and Australo-Antarctica which can be reconciled with the tectonic and topographic response of extension in the Lambert Rift–EARS, Knox Rift, and Wilkes Subglacial Basin (Figure 5a). Furthermore, the formation of high-relief topography in the vicinity of these tectonic structures requires coeval basement exhumation and subsidence in the basins and is incompatible with the concept of large-scale homogenous denudation of East Antarctic basement during the Late Paleozoic Ice Age (~340–300 Ma) proposed by Rolland et al. (2019).

Our thermal modeling results allow modest localized Late Jurassic–Cretaceous cooling of basement in the Bunger Hills region during East Gondwana breakup from palaeotemperatures of ~40°C, which refers to an additional ≤1 km of exhumation in the Denman Glacier area. These estimates do not support significant regional exhumation of a magnitude comparable to the ~4 km Cretaceous exhumation across the Lambert Rift (Arne, 1994; Lisker et al., 2003) and are instead overall consistent with the slow and meager denudation of the low-standing margin segments of the Australo-Antarctic domain as suggested by AFT results reported

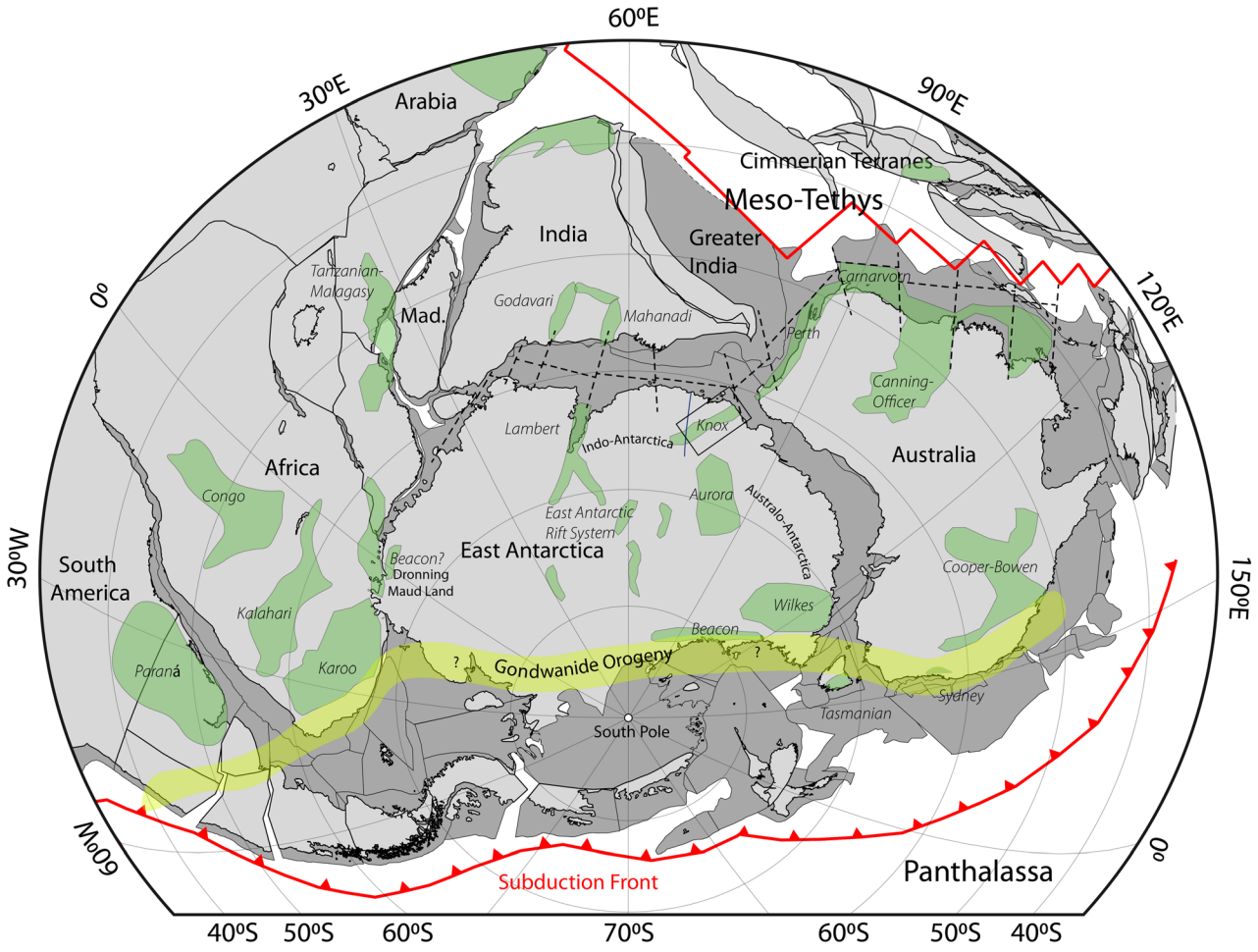

Figure 6. Permian Gondwana tectonic reconstruction (~270 Ma) using GPlates and plate geometries and rotation poles of Matthews et al. (2016). Widespread extensional deformation across the supercontinent was driven by plate convergence along the Panthalassan margin and rifting on the northern margin of Gondwana which resulted in the separation of the Cimmerian Continent and opening of the Meso-Tethys behind it (Metcalfe, 2013). The intracontinental East Gondwanan Late Carboniferous–Triassic rift system (dashed black line; modified from Harrowfield et al., 2005), the distribution of sedimentary basins containing the Pangea Megasequence (green polygons; after Wopfner & Jin, 2009), and the approximate location of the Gondwanide orogenic front (yellow shading) are also shown. The location of the Bunger Hills region and Knox Rift is indicated by the black box.

by Arne et al. (1993) and Lisker and Olesch (2003) (Figure 5b). We therefore suggest that if any significant Cretaceous or younger thermal events between the Bunger Hills region and the TAM occurred, these must be limited in terms of cooling and denudation and therefore not recorded by currently available LTT at the coast.

5.2. Linking Late Paleozoic–Triassic Cooling to Geodynamic Processes and Topographic Relief

The widespread Late Paleozoic–Triassic heating-cooling pattern of East Antarctic basement overlaps with a major phase of thermal instability throughout Pangea marked by geodynamic activity at the periphery of the supercontinent (Frizon de Lamotte et al., 2015). During this time, the propagation of far-field stresses from active plate boundaries resulted in large-scale intracontinental extension and the deposition of ~300–200 Ma Pangea Megasequences in sedimentary basins across all former Gondwana continents (Wopfner & Jin, 2009; Figure 6). We suggest that this phase of extensive intracontinental extension across the hinterland of Gondwana triggered the exhumation of large sections of Precambrian basement in the continental interior of East Antarctica (Figure 5a). Plate convergence along the Panthalassan convergent margin (Veevers & Powell, 1994) led to the deposition of the foreland and back-arc deposits of the Beacon Supergroup in the Wilkes Subglacial Basin (Ferraccioli et al., 2009) and TAM (Elliot, 2013) in Antarctica and the Cooper-Bowen, Sydney (Korsch et al., 2009), and Tasmanian (Fielding et al., 2010) basins of eastern Australia.

Divergence on the northern Gondwana margin resulted in the opening of the Paleo-Tethys Ocean and in the development of a complex Late Carboniferous–Triassic intra-Gondwana rift system (Harrowfield et al., 2005) which includes the Lambert Rift–EARS and Knox Rift together with their Indian (i.e., Mahanadi Basin; Veevers & Tewari, 1995) and Australian (i.e., Perth Basin; Norvick, 2004) conjugate basins. Finally, thermal sag and transtension controlled large Permian–Triassic interior basins like those of central Australia (e.g., Canning and Cooper basins; Wopfner, 1980), subequatorial western Africa (e.g., Congo and Karoo basins; Catuneanu et al., 2005) and South America (e.g., Parana Basin; Zalán et al., 1990). A similar geodynamic origin may be plausible for the broad Aurora Subglacial Basin in the interior of the Australo-Antarctic domain where Late Paleozoic–Mesozoic intracontinental transtension along large-scale faults has been proposed (Aitken, Betts, et al., 2016). Together, these geodynamic processes provide a driver for extensional tectonic activity onshore East Antarctica, which can be reconciled with thermochronological, structural, and stratigraphic evidence supporting widespread Late Paleozoic–Triassic extension. Furthermore, the pattern of ~350–200 Ma AFT and AHe cooling ages on basement highs near Late Paleozoic–Triassic depocenters supports the formation of topographic relief predominantly via differential basement uplift during Late Paleozoic–Triassic intracontinental extension. Low-magnitude denudation of sections of uplifted basement may have also provided sediment sources for intracontinental basins in East Antarctica and on adjacent continents (e.g., Australia; Morón et al., 2019).

While the imprint of Late Paleozoic–Triassic Pangea-wide tectonics is widespread in both the Indo-Antarctic and Australo-Antarctic domains, significant Jurassic–Cretaceous thermal events associated with the breakup of East Gondwana are not equally observed across the two domains (Figure 5b). In the Indo-Antarctic domain, Cretaceous cooling and exhumation of Precambrian basement occurs locally in the Lambert Rift and may be coincident with reactivation of older Late Paleozoic–Triassic structures during large igneous province activity and/or continental rifting between East Antarctica and India (Lisker et al., 2003; Lisker, Gibson, et al., 2007). Geophysical models also predict significant Cretaceous uplift in the interior of the Indo-Antarctic domain along the EARS (Ferraccioli et al., 2011); however, Cretaceous cooling ages are not documented in the offshore detrital LTT record of Prydz Bay (Tochilin et al., 2012), and any significant Cretaceous extensional tectonism in the interior remains therefore poorly constrained. In the Australo-Antarctic domain, onshore Cretaceous–Cenozoic tectonic activity had been suggested on the basis of geophysical data and plate reconstructions (Aitken et al., 2014; Cianfarra & Maggi, 2017; Eagles, 2019; Maritati et al., 2016). However, limited post-Triassic cooling reported across the Australo-Antarctic domain indicates that rifting between Australia and Antarctica did not significantly impact the long-term landscape evolution of the domain and may have only produced local and relatively minor denudational responses (cf. Bunger Hills region).

The record of large-scale topographic evolution driven by Paleozoic–Mesozoic extensional events helps to fill a critical gap in our understanding of the mechanisms responsible for relief variability in the East Antarctic interior. We propose that large-scale variations in amplitude and wavelength of topographic relief across Indo-Antarctica and Australo-Antarctica can largely be accounted for by the effects of intracontinental rifting of Precambrian crust during the Late Paleozoic–Triassic and the subsequent local reactivation of rift structures during Jurassic–Cretaceous breakup of East Gondwana. Phases of continental extension in the Lambert Rift, EARS, and Knox Rift produced narrow rift zones which are responsible for the majority of the high-relief topography that is characteristic of Indo-Antarctic domain and the Bunger Hills region across the transition with the Australo-Antarctic domain. The extensional regime marked by Late Paleozoic–Triassic thermal sag and back-arc extension in most of the Australo-Antarctic domain may instead have led to a more diffuse deformation and the overall low-amplitude long-wavelength topography that characterizes the Australo-Antarctic domain.

5.3. Influence of Tectonic Relief on the Long-Term Landscape Evolution of East Antarctica

The interpreted morphotectonic evolution of the Indo-Antarctic and Australo-Antarctic domains highlights the key role of Paleozoic–Mesozoic tectonic relief in influencing the long-term landscape evolution of East Antarctica. Paleozoic–Mesozoic LTT bedrock ages indicate low long-term erosion rates (10–20 m Ma^{-1}) for uplifted basement highs and suggest the overall preservation of high-standing topographic features at broad wavelengths throughout the Cenozoic (Figure 5c). Subglacial basement highs in the continental interior may also represent tectonically uplifted basement and be characterized by similarly low erosion rates as

suggested by detrital LTT studies (e.g., Cox et al., 2010). Examples of such regions are Highland A in the Aurora Subglacial Basin and Terre Adélie Highlands in Australo-Antarctica, as well as plateau regions such as Princess Elizabeth Land in Indo-Antarctica, all of which can be seen at isostatically rebounded elevations of 1,500–2,000 m (Figure 1b). Flexural models for high-standing bedrock in the Gamburtsev Subglacial Mountains demonstrate that fluvial incision and alpine-style glacial erosion may have also contributed to the long-term landscape evolution of basement highs and be responsible for ~500–700 m of flexural uplift in response to unloading (Paxman et al., 2016). However, the magnitude of cooling and denudation associated with these events is below the detection limit of the AHe and AFT methods, which requires at least 2–3 km of denudation.

Long-term erosion was instead preferentially steered within sedimentary basins, reflecting the strong contrast in erodibility potential between cover sediments and crystalline rocks. However, we suggest that the different morphologies inherited from Late Paleozoic–Triassic extension had a profound influence on the style of erosion. Narrow rifts such as the Lambert and Knox Rifts focused on fluvial and glacial erosion, which caused amplification of topographic relief through selective erosion (Jamieson et al., 2005; Maritati et al., 2016; Thomson et al., 2013) and associated flexural uplift of these structures (Paxman et al., 2016). In contrast, the broad and low-elevation morphology of basins in the central Australo-Antarctic domain allowed for the development of larger fluvial braided systems and river deltas (Paxman, Jamieson, Ferraccioli, et al., 2019; Sauermilch et al., 2019), which provided a substantial amount of detrital material to the Gondwana breakup passive margin basins (Sauermilch et al., 2019). The expansion of the East Antarctic Ice Sheet since the Eocene exacerbated these conditions with high erosion rates (~100 m Ma^{-1}) in the Lambert Rift (Thomson et al., 2013) and dynamic erosion from a marine-based ice sheet in the Aurora (Young et al., 2011) and Wilkes Subglacial Basin (Paxman et al., 2018; Paxman, Jamieson, Ferraccioli, et al., 2019). Together, these observations suggest that tectonic-controlled relief has exerted a key influence on long-term denudation rates and the evolution of the subglacial landscape of East Antarctica, providing a unique example of a continental interior where long-term erosion and associated dynamic responses (i.e., flexure) over millions of years acted to reinforce preexisting topographic relief.

6. Conclusions

We present a model for the origin of topography in the sector of interior East Antarctica between the Lambert Rift and George V Land which establishes a link between Paleozoic–Mesozoic AFT and AHe cooling ages and continent-scale geodynamic processes. We used new ZHe and AHe data from Precambrian basement outcrops to determine the timing, magnitude, and style of Phanerozoic cooling of the Bunger Hills region, a poorly exposed section of East Antarctic basement near the boundary between the two large-scale basement domains of Indo-Antarctica and Australo-Antarctica. Our results indicate that Precambrian basement experienced cooling and ~2–4 km regional exhumation during the Late Paleozoic–Triassic associated with the formation of the Knox Rift, followed by a second episode of localized cooling and $\leq$1 km exhumation associated with the reactivation of rift structures during the Late Jurassic–Cretaceous separation of India from East Gondwana. Late Paleozoic–Triassic cooling and exhumation in the Bunger Hills region is consistent with the timing and magnitude of rift-related cooling and exhumation reported in the Lambert Rift and George V Land, suggesting a single denudational system driven by Pangea-wide extension. We propose that this event had a profound impact on the formation of topographic relief of East Antarctica via the exhumation of large sections of basement and the formation of vast intracontinental sedimentary deposits across the East Antarctic interior. By contrast, extension associated with the Jurassic–Cretaceous breakup of East Gondwana did not provide an equally widespread denudational response across the East Antarctic interior. The topographic framework formed during the Paleozoic–Mesozoic had a significant impact on the long-term landscape evolution of East Antarctica and provided a template for Cenozoic erosion on the continent.

Data Availability Statement

New zircon and apatite (U-Th)/He data are made available in the supporting information (Table S2) and can also be downloaded from the Australian Antarctic Data Centre (following the link https://data.aad.gov.au/metadata/records/AAS_4460_Thermochronology).

Acknowledgments

This research is supported through funding from the Australian Government's Australian Antarctic Program (Project ID 4460) and the Australian Research Council's Special Research Initiative for Antarctic Gateway Partnership (Project ID SR140300001). A. M. is supported by an Australian Government Research Training Program (RTP) Scholarship. M. D. was supported by ARC Discovery funding scheme (DP160102427), the AuScope NCRIS2 program and Curtin Research Fellowship. M. D. acknowledges the help of C. May, C. Scadding, and A. Frew with solution ICP-MS analyses, and I. Dunkl for sharing PepiFLEX software for ICP-MS data reduction. We thank Fausto Ferraccioli and an anonymous reviewer for their constructive criticism and helpful comments which greatly helped improve the manuscript.

References

Aitken, A. R. A., Betts, P. G., Young, D. A., Blankenship, D. D., Roberts, J. L., & Siegert, M. J. (2016). The Australo-Antarctic Columbia to Gondwana transition. *Gondwana Research*, *29*(1), 136–152. https://doi.org/10.1016/j.gr.2014.10.019

Aitken, A. R. A., Roberts, J. L., van Ommen, T. D., Young, D. A., Golledge, N. R., Greenbaum, J. S., et al. (2016). Repeated large-scale retreat and advance of Totten Glacier indicated by inland bed erosion. *Nature*, *533*(7603), 385–389. https://doi.org/10.1038/nature17447

Aitken, A. R. A., Young, D. A., Ferraccioli, F., Betts, P. G., Greenbaum, J. S., Richter, T. G., et al. (2014). The subglacial geology of Wilkes Land, East Antarctica. *Geophysical Research Letters*, *41*, 2390–2400. https://doi.org/10.1002/2014gl059405

Arne, D. C., Kelly, P. R., Brown, R. W., & Gleadow, A. (1993). Reconnaissance apatite fission-track data from the East Antarctic Shield. In *Gondwana symposium* (pp. 605–611).

Arne, D. C. (1994). Phanerozoic exhumation history of northern Prince Charles Mountains (East Antarctica). *Antarctic Science*, *6*(1), 69–84. https://doi.org/10.1017/S0954102094000106

Catuneanu, O., Wopfner, H., Eriksson, P., Cairncross, B., Rubidge, B., Smith, R., & Hancox, P. (2005). The Karoo basins of south-central Africa. *Journal of African Earth Sciences*, *43*(1–3), 211–253. https://doi.org/10.1016/j.jafrearsci.2005.07.007

Cianfarra, P., & Maggi, M. (2017). Cenozoic extension along the reactivated Aurora fault system in the East Antarctic Craton. *Tectonophysics*, *703-704*, 135–143. https://doi.org/10.1016/j.tecto.2017.02.019

Cox, S. E., Thomson, S. N., Reiners, P. W., Hemming, S. R., & van de Flierdt, T. (2010). Extremely low long-term erosion rates around the Gamburtsev Mountains in interior East Antarctica. *Geophysical Research Letters*, *37*, L22307. https://doi.org/10.1029/2010gl045106

Creyts, T. T., Ferraccioli, F., Bell, R. E., Wolovick, M., Corr, H., Rose, K. C., et al. (2014). Freezing of ridges and water networks preserves the Gamburtsev Subglacial Mountains for millions of years. *Geophysical Research Letters*, *41*, 8114–8122. https://doi.org/10.1002/2014GL061491

Daczko, N. R., Halpin, J. A., Fitzsimons, I. C. W., & Whittaker, J. M. (2018). A cryptic Gondwana-forming orogen located in Antarctica. *Scientific Reports*, *8*(1), 8371. https://doi.org/10.1038/s41598-018-26530-1

Eagles, G. (2019). A little spin in the Indian Ocean plate circuit. *Tectonophysics*, *754*, 80–100. https://doi.org/10.1016/j.tecto.2019.01.015

Elliot, D. H. (2013). The geological and tectonic evolution of the Transantarctic Mountains: A review. *Geological Society, London, Special Publications*, *381*(1), 7–35. https://doi.org/10.1144/sp381.14

England, P., & Molnar, P. (1990). Surface uplift, uplift of rocks, and exhumation of rocks. *Geology*, *18*(12), 1173–1177. https://doi.org/10.1130/0091-7613(1990)018<1173:Suuora>2.3.Co;2

Evans, N., Wilson, N., Cline, J., McInnes, B., & Byrne, J. (2005). Fluorite (U–Th)/He thermochronology: Constraints on the low temperature history of Yucca Mountain, Nevada. *Applied Geochemistry*, *20*(6), 1099–1105. https://doi.org/10.1016/j.apgeochem.2005.02.008

Farley, K. (2000). Helium diffusion from apatite: General behavior as illustrated by Durango fluorapatite. *Journal of Geophysical Research*, *105*(B2), 2903–2914. https://doi.org/10.1029/1999JB900348

Farley, K., Wolf, R., & Silver, L. (1996). The effects of long alpha-stopping distances on (U–Th)/He ages. *Geochimica et Cosmochimica Acta*, *60*(21), 4223–4229. https://doi.org/10.1016/S0016-7037(96)00193-7

Ferraccioli, F., Armadillo, E., Jordan, T., Bozzo, E., & Corr, H. (2009). Aeromagnetic exploration over the East Antarctic Ice Sheet: A new view of the Wilkes Subglacial Basin. *Tectonophysics*, *478*(1–2), 62–77. https://doi.org/10.1016/j.tecto.2009.03.013

Ferraccioli, F., Finn, C. A., Jordan, T. A., Bell, R. E., Anderson, L. M., & Damaske, D. (2011). East Antarctic rifting triggers uplift of the Gamburtsev Mountains. *Nature*, *479*(7373), 388–392. https://doi.org/10.1038/nature10566

Fielding, C. R., Frank, T. D., Isbell, J. L., Henry, L. C., & Domack, E. W. (2010). Stratigraphic signature of the late Palaeozoic Ice Age in the Parmeener Supergroup of Tasmania, SE Australia, and inter-regional comparisons. *Palaeogeography, Palaeoclimatology, Palaeoecology*, *298*(1–2), 70–90. https://doi.org/10.1016/j.palaeo.2010.05.023

Frederick, B. C., Young, D. A., Blankenship, D. D., Richter, T. G., Kempf, S. D., Ferraccioli, F., & Siegert, M. J. (2016). Distribution of subglacial sediments across the Wilkes Subglacial Basin, East Antarctica. *Journal of Geophysical Research: Earth Surface*, *121*, 790–813. https://doi.org/10.1002/2015jf003760

Frizon de Lamotte, D., Fourdan, B., Leleu, S., Leparmentier, F., & de Clarens, P. (2015). Style of rifting and the stages of Pangea breakup. *Tectonics*, *34*, 1009–1029. https://doi.org/10.1002/2014tc003760

Harrowfield, M., Holdgate, G. R., Wilson, C. J. L., & McLoughlin, S. (2005). Tectonic significance of the Lambert graben, East Antarctica: Reconstructing the Gondwanan rift. *Geology*, *33*(3), 197. https://doi.org/10.1130/g21081.1

Hu, J., Liu, L., Faccenda, M., Zhou, Q., Fischer, K. M., Marshak, S., & Lundstrom, C. (2018). Modification of the western Gondwana craton by plume–lithosphere interaction. *Nature Geoscience*, *11*(3), 203–210. https://doi.org/10.1038/s41561-018-0064-1

Jamieson, S. S. R., Hulton, N. R. J., Sugden, D. E., Payne, A. J., & Taylor, J. (2005). Cenozoic landscape evolution of the Lambert basin, East Antarctica: The relative role of rivers and ice sheets. *Global and Planetary Change*, *45*(1–3), 35–49. https://doi.org/10.1016/j.gloplacha.2004.09.015

Ketcham, R. A. (2005). Forward and inverse modeling of low-temperature thermochronometry data. *Reviews in Mineralogy and Geochemistry*, *58*(1), 275–314. https://doi.org/10.2138/rmg.2005.58.11

Kohn, B., & Gleadow, A. (2019). Application of low-temperature thermochronology to craton evolution. In M. G. Malusà, & P. G. Fitzgerald (Eds.), *Fission-track thermochronology and its application to geology* (pp. 373–393). Cham: Springer International Publishing. https://doi.org/10.1007/978-3-319-89421-8_21

Korsch, R. J., Totterdell, J. M., Cathro, D. L., & Nicoll, M. G. (2009). Early Permian east Australian rift system. *Australian Journal of Earth Sciences*, *56*(3), 381–400. https://doi.org/10.1080/08120090802698703

Lisker, F., Brown, R., & Fabel, D. (2003). Denudational and thermal history along a transect across the Lambert Graben, northern Prince Charles Mountains, Antarctica, derived from apatite fission track thermochronology. *Tectonics*, *22*(5), 1055. https://doi.org/10.1029/2002TC001477

Lisker, F., Gibson, H., Wilson, C., & Läufer, A. (2007). Denudation and uplift of the Mawson Escarpment (eastern Lambert Graben, Antarctica) as indicated by apatite fission track data and geomorphological observation. *Antarctica. In: Cooper, AK & Raymond, CR (eds) A Keystone in a Changing World–Online Proceedings of the 10th ISAES. USGS Open-File Report, 6*.

Lisker, F., & Olesch, M. (2003). Long-term landscape evolution of George V Land as indicated by fission track data. *Terra Antartica*, *10*(3), 249–256. Retrieved from. https://eurekamag.com/research/019/337/019337137.php

Lisker, F., Wilson, C. J. L., & Gibson, H. J. (2007). Thermal history of the Vestfold Hills (East Antarctica) between Lambert rifting and Gondwana break-up, evidence from apatite fission track data. *Antarctic Science*, *19*(1), 97–106. https://doi.org/10.1017/s0954102007000144

Maritati, A., Aitken, A. R. A., Young, D. A., Roberts, J. L., Blankenship, D. D., & Siegert, M. J. (2016). The tectonic development and erosion of the Knox Subglacial Sedimentary Basin, East Antarctica. *Geophysical Research Letters*, *43*, 10,728–10,737. https://doi.org/10.1002/2016gl071063

Matthews, K. J., Maloney, K. T., Zahirovic, S., Williams, S. E., Seton, M., & Müller, R. D. (2016). Global plate boundary evolution and kinematics since the late Paleozoic. *Global and Planetary Change*, *146*, 226–250. https://doi.org/10.1016/j.gloplacha.2016.10.002

McDowell, F. W., McIntosh, W. C., & Farley, K. A. (2005). A precise ^{40}Ar–^{39}Ar reference age for the Durango apatite (U–Th)/He and fission-track dating standard. *Chemical Geology*, *214*(3–4), 249–263. https://doi.org/10.1016/j.chemgeo.2004.10.002

Metcalfe, I. (2013). Gondwana dispersion and Asian accretion: Tectonic and palaeogeographic evolution of eastern Tethys. *Journal of Asian Earth Sciences*, *66*, 1–33. https://doi.org/10.1016/j.jseaes.2012.12.020

Morlighem, M., Rignot, E., Binder, T., Blankenship, D., Drews, R., Eagles, G., et al. (2020). Deep glacial troughs and stabilizing ridges unveiled beneath the margins of the Antarctic ice sheet. *Nature Geoscience*, *13*(2), 132–137. https://doi.org/10.1038/s41561-019-0510-8

Morón, S., Cawood, P. A., Haines, P. W., Gallagher, S. J., Zahirovic, S., Lewis, C. J., & Moresi, L. (2019). Long-lived transcontinental sediment transport pathways of East Gondwana. *Geology*, *47*(6), 513–516. https://doi.org/10.1130/g45915.1

Mulder, J. A., Halpin, J. A., Daczko, N. R., Orth, K., Meffre, S., Thompson, J. M., & Morrissey, L. J. (2019). A multiproxy provenance approach to uncovering the assembly of East Gondwana in Antarctica. *Geology*, *47*(7), 645–649. https://doi.org/10.1130/g45952.1

Norvick, M. (2004). Tectonic and stratigraphic history of the Perth Basin. *Geoscience Australia Record*, *16*(2004), 30.

O'Donnell, J. P., & Nyblade, A. A. (2014). Antarctica's hypsometry and crustal thickness: Implications for the origin of anomalous topography in East Antarctica. *Earth and Planetary Science Letters*, *388*, 143–155. https://doi.org/10.1016/j.epsl.2013.11.051

Pappa, F., Ebbing, J., Ferraccioli, F., & van der Wal, W. (2019). Modeling satellite gravity gradient data to derive density, temperature, and viscosity structure of the Antarctic lithosphere. *Journal of Geophysical Research: Solid Earth*, *124*, 12,053–12,076. https://doi.org/10.1029/2019JB017997

Paxman, G. J. G., Jamieson, S. S. R., Ferraccioli, F., Bentley, M. J., Ross, N., Armadillo, E., et al. (2018). Bedrock Erosion surfaces record former East Antarctic Ice Sheet extent. *Geophysical Research Letters*, *45*, 4114–4123. https://doi.org/10.1029/2018gl077268

Paxman, G. J. G., Jamieson, S. S. R., Ferraccioli, F., Bentley, M. J., Ross, N., Watts, A. B., et al. (2019). The role of lithospheric flexure in the landscape evolution of the Wilkes Subglacial Basin and Transantarctic Mountains, East Antarctica. *Journal of Geophysical Research: Earth Surface*, *124*, 812–829. https://doi.org/10.1029/2018jf004705

Paxman, G. J. G., Jamieson, S. S. R., Hochmuth, K., Gohl, K., Bentley, M. J., Leitchenkov, G., & Ferraccioli, F. (2019). Reconstructions of Antarctic topography since the Eocene–Oligocene boundary. *Palaeogeography, Palaeoclimatology, Palaeoecology*, *535*, 109346. https://doi.org/10.1016/j.palaeo.2019.109346

Paxman, G. J. G., Watts, A. B., Ferraccioli, F., Jordan, T. A., Bell, R. E., Jamieson, S. S. R., & Finn, C. A. (2016). Erosion-driven uplift in the Gamburtsev Subglacial Mountains of East Antarctica. *Earth and Planetary Science Letters*, *452*, 1–14. https://doi.org/10.1016/j.epsl.2016.07.040

Pinet, N. (2016). Far-field effects of Appalachian orogenesis: A view from the craton. *Geology*, *44*(2), 83–86. https://doi.org/10.1130/g37356.1

Reiners, P. W., Farley, K. A., & Hickes, H. J. (2002). He diffusion and (U–Th)/He thermochronometry of zircon: Initial results from Fish Canyon Tuff and Gold Butte. *Tectonophysics*, *349*(1–4), 297–308. https://doi.org/10.1016/S0040-1951(02)00058-6

Reiners, P. W., Spell, T. L., Nicolescu, S., & Zanetti, K. A. (2004). Zircon (U-Th)/He thermochronometry: He diffusion and comparisons with $^{40}Ar/^{39}Ar$ dating. *Geochimica et Cosmochimica Acta*, *68*(8), 1857–1887. https://doi.org/10.1016/j.gca.2003.10.021

Rolland, Y., Bernet, M., van der Beek, P., Gautheron, C., Duclaux, G., Bascou, J., et al. (2019). Late Paleozoic ice age glaciers shaped East Antarctica landscape. *Earth and Planetary Science Letters*, *506*, 123–133. https://doi.org/10.1016/j.epsl.2018.10.044

Sauermilch, I., Whittaker, J. M., Bijl, P. K., Totterdell, J. M., & Jokat, W. (2019). Tectonic, oceanographic, and climatic controls on the cretaceous-Cenozoic sedimentary record of the Australian-Antarctic Basin. *Journal of Geophysical Research: Solid Earth*, *124*, 7699–7724. https://doi.org/10.1029/2018JB016683

Thomson, S. N., Reiners, P. W., Hemming, S. R., & Gehrels, G. E. (2013). The contribution of glacial erosion to shaping the hidden landscape of East Antarctica. *Nature Geoscience*, *6*(3), 203–207. https://doi.org/10.1038/ngeo1722

Tochilin, C. J., Reiners, P. W., Thomson, S. N., Gehrels, G. E., Hemming, S. R., & Pierce, E. L. (2012). Erosional history of the Prydz Bay sector of East Antarctica from detrital apatite and zircon geo- and thermochronology multidating. *Geochemistry, Geophysics, Geosystems*, *13*, Q11015. https://doi.org/10.1029/2012gc004364

Tucker, N. M., Hand, M., & Clark, C. (2020). The Bunger Hills: 60 years of geological and geophysical research. *Antarctic Science*, *32*(2), 85–106. https://doi.org/10.1017/s0954102019000403

Veevers, J. J. (2018). Gamburtsev Subglacial Mountains: Age and composition from morainal clasts and U–Pb and Hf-isotopic analysis of detrital zircons in the Lambert Rift, and potential provenance of east Gondwanaland sediments. *Earth-Science Reviews*, *180*, 206–257. https://doi.org/10.1016/j.earscirev.2018.03.002

Veevers, J. J., & Powell, C. M. (1994). Permian-Triassic Pangean basins and foldbelts along the Panthalassan margin of Gondwanaland (Vol. 184): Geological Society of America.

Veevers, J. J., & Tewari, R. C. (1995). Gondwana master basin of Peninsular India between Tethys and the interior of the Gondwanaland Province of Pangea. In J. J. Veevers & R. C. Tewari (Eds.), (Vol. 187, pp. 0): Geological Society of America.

Wagner, G., Gleadow, A., & Fitzgerald, P. (1989). The significance of the annealing zone in apatite fission-track analysis: Projected track length measurements and uplift chronology of the Transantarctic Mountains. *Chemical Geology: Isotope Geoscience Section*, *79*(4), 295–305.

Weber, U. D., Kohn, B. P., Gleadow, A. J. W., & Nelson, D. R. (2005). Low temperature Phanerozoic history of the northern Yilgarn Craton, Western Australia. *Tectonophysics*, *400*(1–4), 127–151. https://doi.org/10.1016/j.tecto.2005.03.008

Wildman, M., Brown, R., Beucher, R., Persano, C., Stuart, F., Gallagher, K., et al. (2016). The chronology and tectonic style of landscape evolution along the elevated Atlantic continental margin of South Africa resolved by joint apatite fission track and (U-Th-Sm)/He thermochronology. *Tectonics*, *35*, 511–545. https://doi.org/10.1002/2015tc004042

Wopfner, H. (1980). Development of Permian intracratonic basins in Australia. Paper Presented at the Gondwana Five. Proceedings of the Fifth International Gondwana Symposium, Wellington, New Zealand.

Wopfner, H., & Jin, X. C. (2009). Pangea Megasequences of Tethyan Gondwana-margin reflect global changes of climate and tectonism in Late Palaeozoic and Early Triassic times—A review. *Palaeoworld*, *18*(2–3), 169–192. https://doi.org/10.1016/j.palwor.2009.04.007

Young, D. A., Wright, A. P., Roberts, J. L., Warner, R. C., Young, N. W., Greenbaum, J. S., et al. (2011). A dynamic early East Antarctic Ice Sheet suggested by ice-covered fjord landscapes. *Nature*, *474*(7349), 72–75. Retrieved from. https://doi.org/10.1038/nature10114

Zalán, P. V., Wolff, S., Astolfi, M. A. M., Vieira, I. S., Concelcao, J. C. J., Appi, V. T., et al. (1990). The Parana Basin, Brazil: Chapter 33: Part II. Selected Analog Interior Cratonic Basins: Analog Basins.